In situ surface pH measurement during electrolysis using a rotating pH electrode

by H. Deligianni
L. T. Romankiw

An *in situ* technique has been developed for measuring the surface pH adjacent to a solid electrode/liquid interface during electrolysis. Measurements of the surface pH can be used to obtain insights regarding the electrodeposition of various transition metals and to obtain a better understanding of associated *in situ* surface chemistry effects. Many transition metals and alloys deposit with simultaneous hydrogen evolution and, as a result, are accompanied by a pH rise near the cathode, thereby affecting the reactivity of the nearby metal-ion species. Measurements of the surface pH of a solution containing simple salts during hydrogen evolution from a cathode were performed. The surface pH of a cathode during Ni and NiFe electrodeposition was also measured. The experiments demonstrated that, in the absence of buffers or metal ions, the surface pH rises many pH units above the bulk value. During Ni and NiFe electrodeposition, however, the surface pH of solutions consisting of simple salts and starting from a bulk pH level of 2 does not increase more than 3 pH units from the bulk value. In the case of Ni and NiFe electrodeposition, surface buffering occurs because of the hydrolysis of the metal-ion species present. Additionally, it is found that during the anomalous codeposition of NiFe, the surface pH is much lower than that required by the Dahms–Croll hypothesis.

Introduction

Typically two electrodes separated by an electrolyte phase constitute an electrochemical cell [1]. Electrode reactions are interfacial reactions and occur in a region called the double layer, extending 10–100 Å away from the solid surface. Concentration changes of ionic species in the liquid phase typically occur in a region which extends a few microns away from the electrode and within the diffusion layer. The thickness of the diffusion layer can be adjusted by judicious control of the hydrodynamic conditions of the system. In this work, a technique is described for the localized measurement of the pH within the diffusion layer during electrolysis under conditions of controlled agitation. It is shown here that metal-ion hydrolyzed species act as buffering agents to suppress the localized pH rise. Their role in the mechanism of metal electrodeposition is discussed.

Table 1 lists selected standard electrode potentials in aqueous solutions. The more negative the standard electrode potential, the more difficult it is to deposit the indicated metal. Reactions that have a more negative standard electrode potential than hydrogen ($2H^+ + 2e^- \rightarrow H_2$) deposit with evolution of hydrogen as a side reaction. Electrodeposition of most of the non-noble metals such as Ni, Fe, Co, and Zn are accompanied by H_2 evolution.

Typical reactions which may take place during the deposition of metals having a negative standard electrode potential are as follows:

$$M^{+n} + ne^- \rightleftarrows M \qquad \text{Metal deposition} \qquad (1)$$

$$2H^+ + 2e^- \rightleftarrows H_2 \qquad \text{Hydrogen evolution} \qquad (2)$$

$$2H_2O + 2e^- \rightleftarrows H_2 + 2OH^- \qquad \text{Water decomposition} \qquad (3)$$

$$xM^{+n} + yH_2O \rightleftarrows M_x\,(OH)y^{(xn-y)+} + yH^+ \qquad \text{Hydrolysis of metal ion} \qquad (4)$$

$$xM_x\,(OH)_y^{(xn-y)+} + (xn-y)\,H_2O \rightleftarrows xM\,(OH)_n + (xn-y)\,H^+ \qquad \text{Precipitation of hydroxide} \qquad (5)$$

Electrochemical reactions (2) and (3) tend to consume H^+ or generate OH^-. Hence, when they take place at the cathode, the pH of the cathode will increase. Reactions (4) and (5) tend to produce H^+ and will counteract the pH rise at the cathode produced by reactions (2) and (3). When the pH near the surface becomes such that hydrolysis and precipitation reactions occur, any further pH rise will be slowed by reactions (4) and (5). If the hydrolysis reaction (4) is not able to slow the pH rise, the deposit may contain hydroxide inclusions because of reaction (5).

Our technique makes it possible to carry out nondestructive, noninvasive surface pH measurements and facilitates the characterization of the chemical processes that occur near the surface during electrodeposition. The phenomenon of pH rise at the cathode during electroplating is found to affect the reaction mechanisms of metal and alloy electrodeposition and the structure and properties of the associated electrodeposits.

The changes of pH at the cathode during electroplating of transition metals and alloys have been studied by many investigators [2–21]. Kuhn and Chan [2] have presented a review of different techniques by which near-surface pH levels have been measured. Eastham and Boden [3] used a method of rapid freezing of the electrolyte involving shaving thin frozen layers and measuring the pH of these layers. Matulis and Slizys [4] measured pH changes as a function of the distance from the cathode by placing glass microelectrodes at preselected distances from the electrode surface during Ni electrodeposition. Despite the difficulty of reproducible placement of microelectrodes and the disturbance these may cause to the potential and transport fields, both studies suggested that Ni electrodeposition proceeds via a nickel monohydroxy species ($NiOH^+$) and that the surface pH may reach values at which nickel hydroxide [$Ni(OH)_2$] would precipitate at the surface and would inhibit metal deposition. Kublanowski [5] experienced reproducibility problems with the use of antimony and bismuth electrodes because of the ease of poisoning of these microelectrodes by the electrolyte used in electroplating.

Brenner [6] and subsequently Knoedler and Neugebohren [7] used a suck-off technique in which a small sample of the liquid electrolyte was withdrawn in order to measure pH, and were quite effective in demonstrating that there is a large increase in the pH level at the cathode during electroplating. However, withdrawal of even a small volume of solution disturbs the buildup of species concentration and affects the accuracy and reproducibility of the measurements.

Harris [8] developed a mathematical model which predicted hydroxyl ion of OH^- concentrations in the diffusion layer during the deposition of a bivalent metal. On the basis of a proposed model, he concluded that the degree of cathode alkalization depends on the rate of H^+ consumption at the cathode, buffering reactions in the diffusion layer, and complexation reactions of the metallic ions with the anions present.

Dahms and Croll [9] were the first to stress the importance of surface pH during NiFe electrodeposition. Their work was aimed at explaining the mechanism of NiFe anomalous codeposition in which, contrary to the expected, preferred deposition of nickel, iron deposits preferentially to Ni from the Ni-Fe solutions. It is necessary to have as much as 80:1 molar Ni/Fe ratio in solution to achieve a Ni/Fe ratio of 4:1 in the film. Dahms and Croll concluded that the anomalous NiFe deposition occurs when the limiting current for hydrogen evolution is exceeded, and that the formation of ferrous hydroxide at the electrode surface can inhibit the nickel deposition reaction. They developed a model for predicting the pH change at the cathode and showed that in solutions of Ni and Fe, the pH at the cathode increases from the initial value of 2.5 to values as high as 8 or 9.

Castellani et al. [10] and Powers and Romankiw [11], using a paddle cell, and Andricacos et al. [12], using a ring-disk electrode, demonstrated that agitation plays a significant role in controlling NiFe deposition. Recently, Hessami and Tobias [13] have developed a model for predicting the anomalous behavior of NiFe codeposition. The model is based on the hypothesis that hydrolyzed Ni^{+2} and Fe^{+2} species ($NiOH^+$, $FeOH^+$) adsorb at the electrode surface and compete for surface active sites. Comparison between the predictions of the model and the experimental work of Andricacos et al. [12] has shown good qualitative agreement.

The pH measurement technique described in this paper has been demonstrated to be simple, reproducible, and reliable. It was first developed by Romankiw [14–17] in order to verify the predictions of Dahms and Croll [9]. Deligianni and Romankiw [18, 19] used the technique to gain further insight into the effect of individual solution components in Ni [18] and NiFe plating solutions [19]. Most recently, Deligianni and Romankiw [20–22] have developed a rotating pH electrode capable of measuring *in situ* surface pH under well-controlled hydrodynamic conditions. In this paper, pH measurements both in the absence of metal ions and during Ni and NiFe electrodeposition are reported.

Description of experimental apparatus and technique

The technique makes use of a flat-bottomed glass electrode positioned at the back of a very thin metal screen cathode, as shown in **Figure 1** in cross section. A very thin metal screen with small, uniform-sized apertures is brought into intimate contact with a flat-bottomed glass pH electrode. When the screen is used as a cathode, the pH glass electrode registers an average of the pH changes which occur within the apertures. Since the measurement is made simultaneously in hundreds of apertures, the signal is large, and the signal-to-noise ratio is also large. Neither the electrical field nor the transport field is disturbed by the glass electrode. If the screen is very thin and the apertures are very small in comparison to the diffusion layer thickness of H^+ ions, it is possible to measure a pH value which is close to the actual pH value at the cathode surface. If more precise values are desired, it is necessary to carry out experiments involving a series of metal screens which have progressively smaller apertures and which are progressively thinner, thus arriving at the pH value of the electrode by extrapolation (shown in

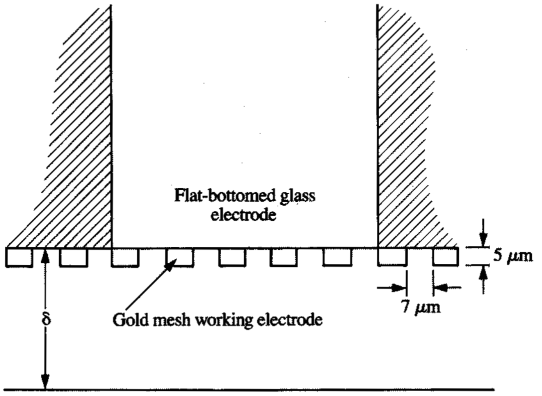

Figure 1

Cross section of a thin metal screen pressed against a flat-bottomed glass pH electrode. The thin metal screen is used as a cathode. The surface pH is registered by the pH electrode through the holes of the mesh. In order to obtain accurate measurements in the presence of agitation, the size of the mesh apertures must be smaller than the thickness of the diffusion layer.

Table 1 Selected standard electrode potentials in aqueous solutions at 25°C.

Reaction	$E_{25°C}$ (V vs. NHE)
$Li^+ + e^- \rightarrow Li$	−3.010
$Ca^{2+} + 2e^- \rightarrow Ca$	−2.860
$Mg^{2+} + 2e^- \rightarrow Mg$	−2.360
$Ti^{2+} + 2e^- \rightarrow Ti$	−1.750
$Al^{3+} + 3e^- \rightarrow Al$	−1.662
$Zn^{2+} + 2e^- \rightarrow Zn$	−0.762
$Cr^{3+} + 3e^- \rightarrow Cr$	−0.744
$Fe^{2+} + 2e^- \rightarrow Fe$	−0.447
$Cd^{2+} + 2e^- \rightarrow Cd$	−0.403
$Co^{2+} + 2e^- \rightarrow Co$	−0.280
$Ni^{2+} + 2e^- \rightarrow Ni$	−0.257
$Mo^{3+} + 3e^- \rightarrow Mo$	−0.200
$Sn^{2+} + 2e^- \rightarrow Sn$	−0.137
$Pb^{2+} + 2e^- \rightarrow Pd$	−0.126
$H^+ + e^- \rightarrow 1/2H_2$	+0.000
$Cu^{2+} + 2e^- \rightarrow Cu$	+0.342
$Te^{2+} + 4e^- \rightarrow Te$	+0.568
$PdCl_4^{2-} + 2e^- \rightarrow Pd + 4Cl^-$	+0.591
$Ag^+ + e^- \rightarrow Ag$	+0.799
$Au^+ + e^- \rightarrow Au$	+1.692

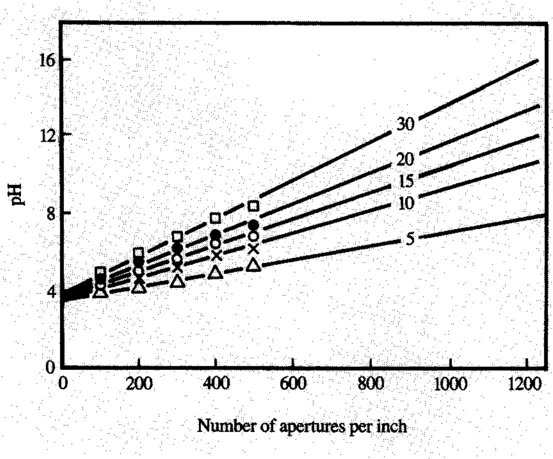

Figure 2

pH values plotted as a function of the number of apertures per inch for different total applied currents through the mesh. Total currents (in mA) are indicated. The screen dimensions were 1 in. by 1 in. by 0.5 in. From [14], reprinted by permission of the publisher, The Electrochemical Society, Inc.

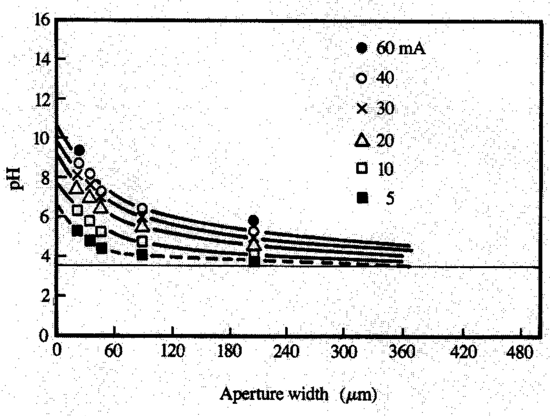

Figure 3

A plot of the same data as in Figure 2, except that the mesh values have been replaced by the actual widths of the apertures in the different screens used. As the aperture width decreases, the measured pH change for a given current increases and can be extrapolated to the pH at the surface of the glass electrode. From [14], reprinted by permission of the publisher, The Electrochemical Society, Inc.

Figures 2, 3). In this study, a fine mesh screen of Ni or Au with 2000 lines per inch pressed against a flat-bottomed combination electrode was used. The screen contained 7-μm-wide apertures and was 2.5 μm thick (2000-mesh screen).

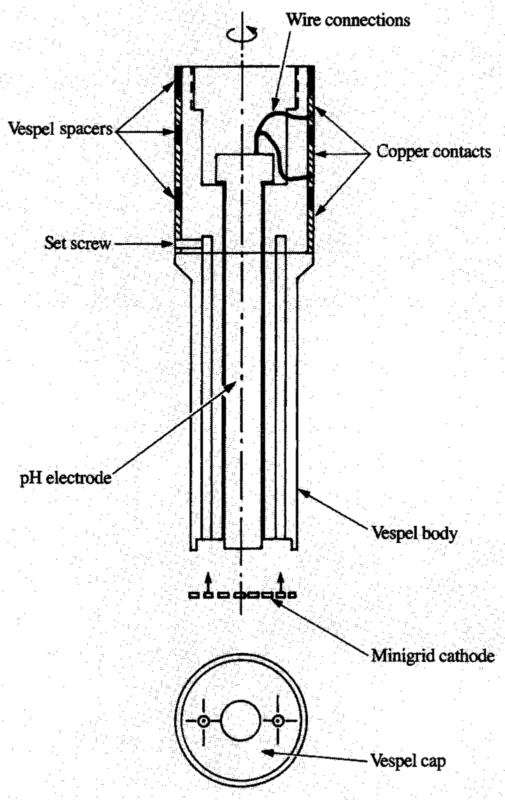

Figure 4

Rotating pH electrode assembly for surface pH measurements in the presence of agitation. From [21], reprinted by permission of the publisher, The Electrochemical Society, Inc.

The assembly for *in situ* pH measurements under conditions of controlled agitation is shown in **Figure 4.** It consists of a housing of Vespel. A flat-surface pH electrode fits inside the housing. The pH electrode is connected to two wires soldered onto two copper rings surrounding the housing. The copper rings are in turn in contact with carbon brushes (not shown in Figure 4), providing electrical connection to the pH meter and permitting measurement of pH levels. A third copper ring is used for electrical contact to the working electrode. Set screws bring the copper ring in contact with copper rods, against which a fine mesh gold or nickel screen electrode is pressed. The fine mesh is placed in the recess formed at one end of the housing and is in contact with the pH electrode. A Pt screen immersed in the same glass container as the working electrode is used as counter electrode. An ORION Ag/AgCl electrode was used as the reference electrode. The flat-bottomed pH electrode was calibrated prior to use using standard solutions of pH 4 and pH 7. Use was made of a CORNING 240 pH meter to measure pH levels. The electrode potential was controlled with an AMEL 555B potentiostat. Outputs of the pH meter in millivolts, the current, and the cathode potential were stored in a NICOLET Model 4094B digital oscilloscope having Model 4851 plug-in modules. Measurements of near-surface pH as a function of potential were carried out on each solution component separately and then on the solution constituents in combination. Chloride-based solutions acidified to pH 2 and 3 with HCl were used. A solution containing 0.2 M $NiCl_2$, 5 mM $FeCl_2$, and 0.4 M NaCl was used. Some of the solutions also contained 0.4 M H_3BO_3. The solutions were prepared immediately prior to use.

Surface pH during hydrogen evolution in the absence of metal ions

A salt solution (0.8 M NaCl) was used as a supporting electrolyte to evolve H_2 on a Ni electrode surface. It is expected that, under these conditions, H_2 will be evolved by reactions (2) and (3) and thus the surface pH will be very alkaline. Measurements of surface pH during H_2 evolution on a Ni electrode from a 0.8 M NaCl solution are shown in **Figure 5**. The surface pH reached values of 11 and 10.5 at rotation speeds of 100 and 400 rpm, respectively. The surface pH measured at 400 rpm tends to increase much more slowly than the surface pH at 100 rpm because of the much higher rate of H^+ supply to the surface at higher rotation speeds. In a stagnant solution it is expected that the surface pH will reach values close to 13–14.

The logarithm of current versus potential for H_2 evolution on a Ni screen used as a cathode, as a function of rotation speed, is shown in **Figure 6**. Evolution of H_2 on a metal consists of reactions (2) and (3). The limiting current plateau for H^+ reduction in an 0.8 M NaCl solution increases with rotation speed. The limiting current plateau occurs in the potential region of −800 to −1300 vs. Ag/AgCl. As shown in Figure 5, appreciable pH changes are observed at potentials corresponding to the H^+ limiting current. At more cathodic (negative) potentials, the current increases even more because of the water decomposition reaction [reaction (3)].

It is known that H_3BO_3 (boric acid) is a weak acid at low concentrations with a pK value of 9; at concentrations higher than 22 mM it tends to polymerize and dissociate, with a pK value of 6.84 [23]. Typically, Permalloy solutions contain 0.4 M H_3BO_3, and thus a pK value of 6.84 can be used.

There has long been a controversy in the literature on the role of boric acid in plating solutions. This paper will try to shed light on this subject. Figure 5 shows the measured surface pH as a function of potential in a solution containing 0.4 M H_3BO_3 and 0.4 M NaCl. In the presence of boric acid, Figure 5 shows that the surface pH reaches values of 6.5 and 5.5 at 100 rpm and 400 rpm. On the basis of the pK value of 6.84, a 0.4 M H_3BO_3 should buffer at a pH of about 4. However, such an effect is not

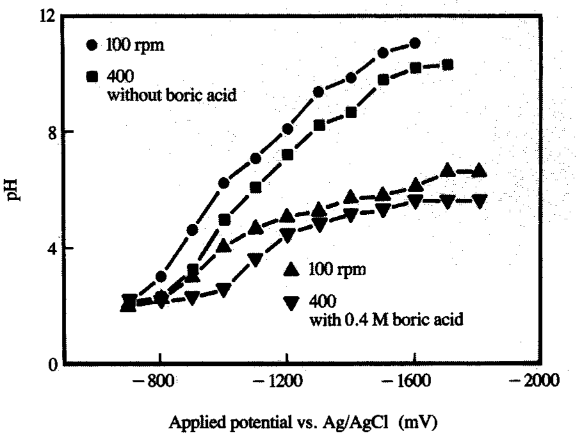

Figure 5

Near-surface pH as a function of applied potential during H_2 evolution on a Ni electrode. Solutions contained 0.8 M NaCl or 0.4 M NaCl and 0.4 M H_3BO_3 at a pH of 2.

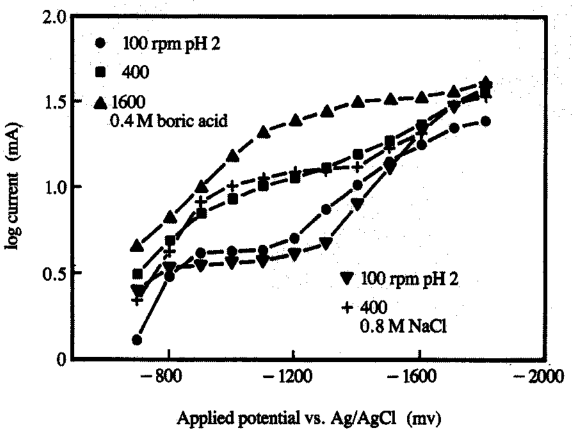

Figure 6

Potentiostatic curves for a Ni electrode evolving H_2. Solution compositions same as those of Figure 5.

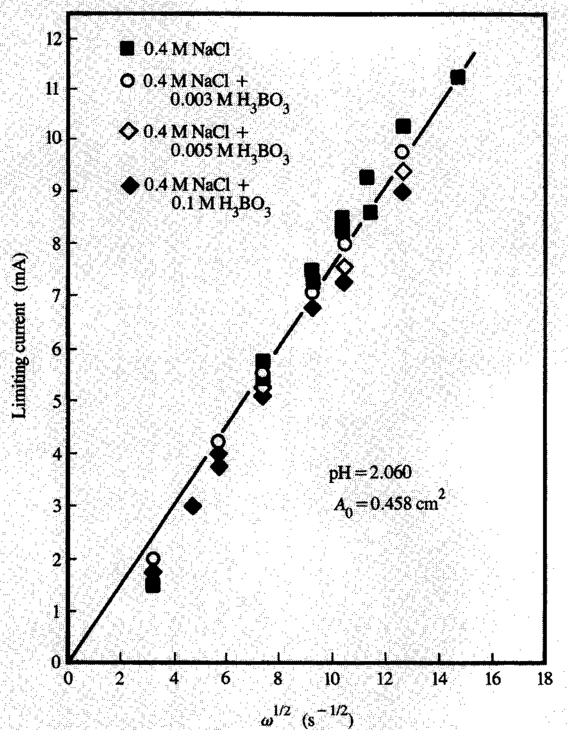

Figure 7

Limiting current of H^+ reduction on a Pt disk electrode as a function of the square root of rotation frequency ω.

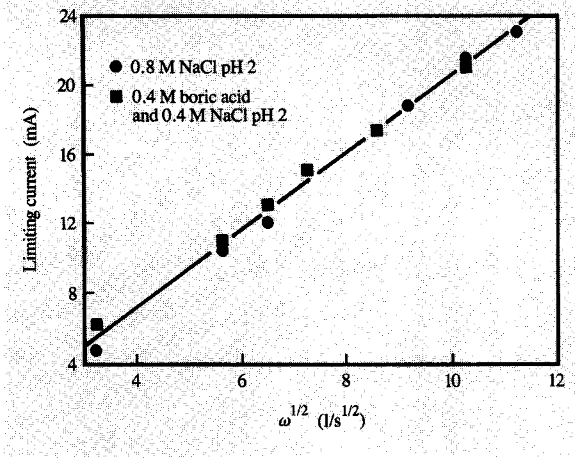

Figure 8

Limiting current of H^+ reduction on a Ni mesh electrode as a function of the square root of rotation frequency.

seen in Figure 5. On the other hand, the limiting current plateau of H^+ reduction does not change in the presence of H_3BO_3 in solution, as seen in **Figure 7**. If the H_3BO_3 acid acted as a buffer, it would increase the limiting current of H^+ reduction (Figures 6 and 7) and would also buffer at a pH of 4, resulting in a pH plateau. In addition, it is observed from Figure 6 that boric acid moves the water decomposition reaction to more noble potentials. This study confirms these observations, which were previously made by Horkans [24]. Although boric acid may not act as a typical buffer, it must have an inhibiting effect on hydrogen evolution because, when present, it reduces the surface pH (Figure 5).

The limiting current I_l for H^+ reduction on a Pt disk electrode as a function of the square root of rotation frequency is shown in Figure 7. As can be seen, it follows the Levich equation of mass transport on a rotating disk electrode:

$$I_l = 0.62nFDC_b A_0^{2/3} v^{-1/16}\, \omega^{1/2}, \tag{6}$$

where C_b is the bulk concentration of H^+ (gmol/cm^3), A_0 is the disk area (cm^2), D is the diffusion coefficient of H^+ (cm^2/s), v is the solution kinematic viscosity (cm^2/s), and ω is the rotation frequency (1/s).

The diffusion coefficient of H^+ was calculated from the slope of Equation (6) and was found to be 5.79×10^{-5} cm^2/s. This value compares well with literature values.

From the slope of the line in **Figure 8**, the area of the 2000-mesh electrode used to obtain the limiting current data was calculated to be equal to the area of a flat-surface electrode. A 2000-mesh electrode behaves as a flat surface because the apertures are so small that they hardly create a disturbance in the transport field.

Surface pH during nickel electrodeposition

The near-surface pH was examined as a function of potential for Ni deposition via different $NiCl_2$ concentrations in the absence of buffering agents; the results obtained are shown in **Figure 9**. Hydrogen evolution on Au from a 1 M NaCl solution was used as a reference (curve a). In a 1 M NaCl solution, the pH at the surface increased up to a value of 13. When 5 mM $NiCl_2$ was added to the solution, the surface pH reached a value of 12 (curve b). Curves c, d, and e correspond to solutions containing the supporting electrolyte and 10 mM, 0.1 M, and 0.2 M $NiCl_2$, respectively. For a constant applied potential the pH change at the surface decreased as the amount of $NiCl_2$ increased.

It is evident from Figure 9 that the curves representing surface pH versus potential exhibit a plateau on which the pH is independent of applied electrode potential. The plateau appears to correspond to hydrolysis of Ni^{+2} ions to monohydroxy ($NiOH^+$) and polymeric hydrolyzed species such as $Ni_2(OH)^{+3}$ and $Ni_4(OH)_4^{+4}$. To check this, a simple

Table 2 Comparison between measured and calculated hydrolysis pH values as a function of $NiCl_2$ concentration.

$Ni^{2+} + H_2O = NiOH^+ + H^+$		$K_{eq} = \frac{NiOH^+H^+}{Ni^{2+}}$
$NiCl_2$ (mM)	*Measured*	*Calculated* (from K_{eq})
200	4.50	5.27
100	5.00	5.42
10	6.00	5.92

calculation was made in which only the monohydroxy Ni species was considered, i.e., $NiOH^+$. The hydrolysis equilibrium constant of Ni^{+n} was taken from Baes and Mesmer [23] to be $10^{-9.84}$. At a given potential, the H^+ concentration at the pH plateau minus the H^+ concentration of the H_2 evolution reaction should give the amount of H^+ produced by hydrolysis. The pH values resulting from the hydrolysis reaction were calculated for every $NiCl_2$ concentration and were compared with measured values. **Table 2** shows that the agreement between the calculated and measured pH values was good.

For curve e of Figure 9, at a potential of −1600 mV vs. Ag/AgCl, the pH value reaches a level of 8.5. At this point the resulting deposit appears black. On the basis of Ni^{+2} solubility (solubility product: 10^{-16}) under these conditions, one would expect precipitation of nickel hydroxide. To investigate the nature of the black deposit, deposition was carried out in the potentiostatic mode at −1600 mV vs. Ag/AgCl, and the resulting 5-μm-thick deposit was analyzed by Auger electron spectroscopy (AES). **Figure 10** shows a depth profile of the deposit, sputtered to a depth of 3600 Å. It was found that the deposit consisted of Ni, O, and Cl, suggesting precipitation and inclusion of $Ni(OH)_xCl_y$ at the electrode during Ni electrodeposition from $NiCl_2$ salts. Subsequently, deposition was performed in a 0.2 M $NiSO_4$ electrolyte. Auger profiling to a depth of 960 Å (**Figure 11**) revealed that the deposit consisted of equal amounts of Ni and O, suggesting that in the absence of Cl^- only $Ni(OH)_2$ precipitates at the electrode.

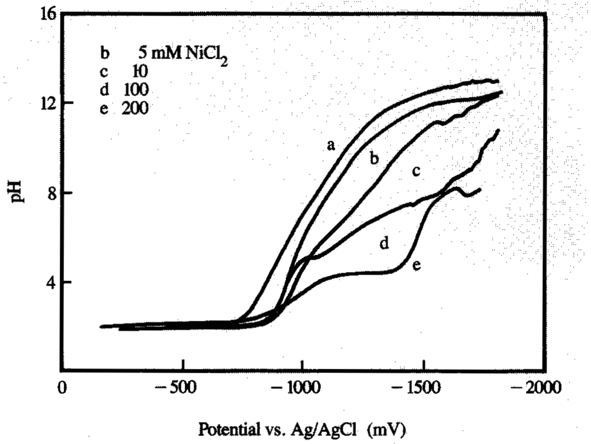

Figure 9

Near-surface pH as a function of applied potential for Ni deposition: curve a, H_2 evolution on Au in 1 M NaCl; curves b–e, Ni deposition from solutions containing 5, 10, 100, and 200 mM $NiCl_2$ with NaCl to an ionic strength of 1 and a bulk pH of 2. The sweep rate was 1 mV/s. From [18], reprinted by permission of the publisher, The Electrochemical Society, Inc.

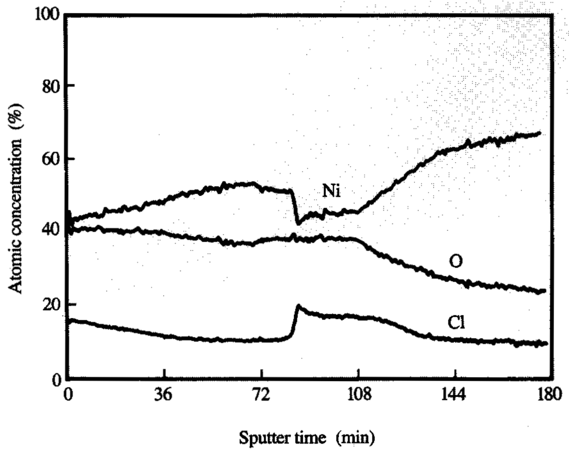

Figure 10

AES depth profile of deposit obtained at −1600 mV vs. Ag/AgCl from a 0.2 M $NiCl_2$ solution having a bulk pH of 2. From [18], reprinted by permission of the publisher, The Electrochemical Society, Inc.

The effect of agitation on the surface pH during Ni electrodeposition from a 0.2 M $NiCl_2$ solution is shown in **Figure 12.** As the rotation frequency is increased in steps from 100 rpm to 1600 rpm, the surface pH rise in the diffusion layer is suppressed. The same behavior was exhibited by the H_2 evolution reaction. At 1600 rpm the surface pH increases by only one pH unit from the initial pH value and at potentials as cathodic as −1500 mV. The measurements shown in Figure 5 and the work by Andricacos et al. [12] show that over the potential region of Ni and NiFe deposition, H^+ reduction is influenced by mass transfer and therefore is strongly dependent on agitation. With increased agitation, the H^+ supply to the electrode is faster, thus keeping the surface pH closer to

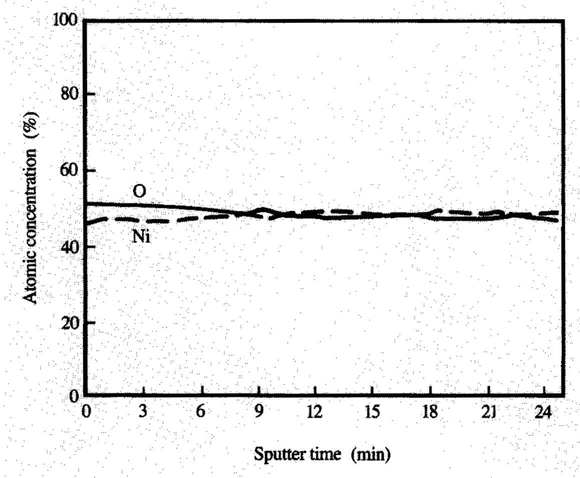

Figure 11

AES depth profile of deposit obtained at −1600 mV vs. Ag/AgCl from a 0.2 M $NiSO_4$ solution having a bulk pH of 2. From [18], reprinted by permission of the publisher, the Electrochemical Society, Inc.

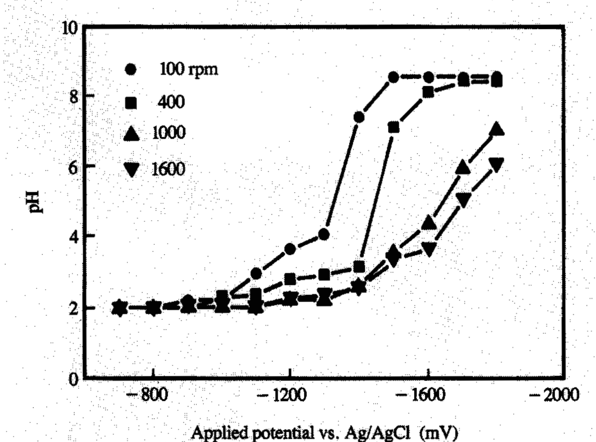

Figure 12

Effect of agitation on near-surface pH for Ni deposition from a solution containing $NiCl_2$ and 0.4 M NaCl having a bulk pH of 2. From [21], reprinted by permission of the publisher, The Electrochemical Society, Inc.

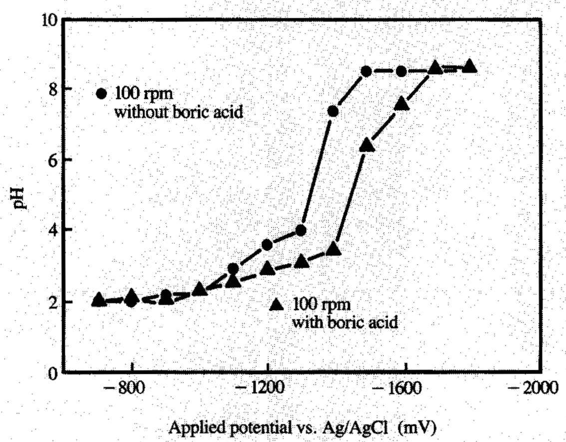

Figure 13

Effect of presence of boric acid on surface pH during Ni electrodeposition from a solution containing 0.2 M $NiCl_2$, 0.4 M H_3BO_3, and 0.4 M NaCl, and having a bulk pH of 2.

that of the bulk value. However, the surface pH during Ni electrodeposition is appreciably lower than the pH during H_2 evolution in the absence of metal ions. In addition, the pH-vs.-potential curves during Ni electrodeposition exhibit a pH plateau. Both the lower pH values and the pH plateau, which is independent of electrode potential, suggest that during Ni deposition, hydrolysis of Ni^{+2} ions and the accompanying additional generation of H^+ take place next to the cathode surface. Furthermore, due to the fact that vigorous agitation maintains a low surface pH, precipitation of hydroxides is impeded even at very high cathodic potentials. For example, at 1600 rpm, precipitation of $Ni(OH)_xCl_y$ does not occur even at −1800 mV vs. Ag/AgCl. Deposits obtained at 1600 rpm have a shiny metallic appearance because the surface pH is kept at low levels. Therefore, by measuring the surface pH, it is possible to predict the appearance of deposits and develop control over their quality.

Current efficiency is defined as the ratio of the current used for metal electrodeposition to the total current used for all electrode reactions. For example, in the case of Ni electrodeposition, the only side-reaction is hydrogen evolution; a 70% level in current efficiency implies that 70% of the total current is used to electrodeposit the Ni and 30% is used for generating hydrogen. When boric acid is present in a Ni-containing solution, the surface pH is even lower than in the absence of boric acid (**Figure 13**). However, its presence increases the current efficiency for Ni deposition, as is evident from the results presented in **Figure 14**, indicating that its presence suppresses H_2 evolution from the Ni surface. The exact mechanism of

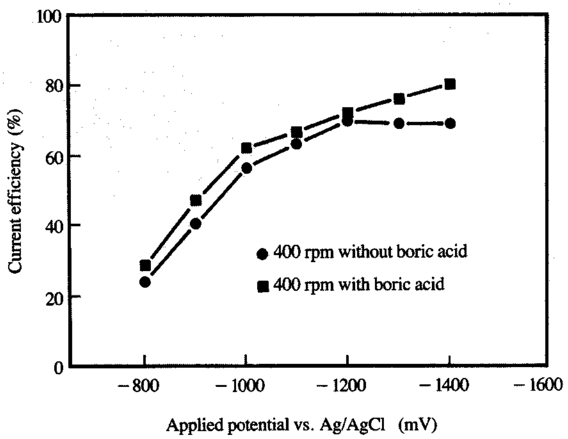

Figure 14

Effect of boric acid on current efficiency for Ni electrodeposition from a solution containing 0.2 M $NiCl_2$, 0.4 M H_3BO_3, and 0.4 M NaCl, and having a bulk pH of 2.

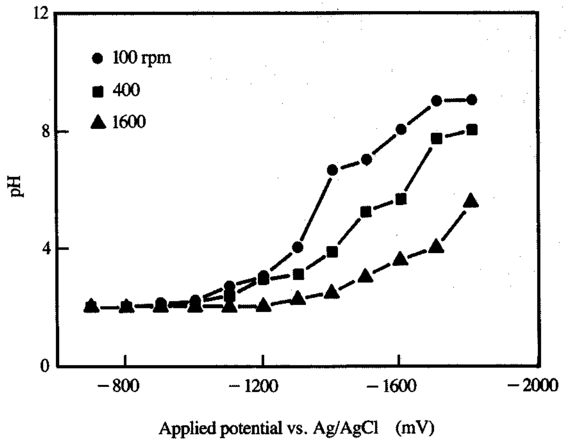

Figure 15

Effect of agitation on the surface pH during NiFe electrodeposition from a solution containing 0.2 M $NiCl_2$, 5 mM $FeCl_2$, and 0.4 M NaCl, and having a bulk pH of 2. From [21], reprinted by permission of the publisher, The Electrochemical Society, Inc.

hydrogen evolution inhibition can be postulated to occur through adsorption of boric acid on surface-active sites.

Surface pH during nickel iron electrodeposition

The effect of agitation on the surface pH during NiFe electrodeposition from a 0.2 M $NiCl_2$, 5 mM $FeCl_2$, 0.4 M NaCl solution having a bulk pH of 2 is shown in **Figure 15**. An interesting observation from this figure is that at 1600 rpm there is hardly any pH rise at the surface. The potential range between −800 mV and −1300 mV vs. Ag/AgCl is typical of the potential range in which Permalloy (NiFe) is usually deposited. By comparison to Figure 12, which shows the surface pH during Ni deposition, the surface pH in the potential region of interest is much lower. This suggests additional buffering effects at the surface resulting from the presence of hydrolyzed ferrous species. As a result, the measured surface pH is much lower than that required by the Dahms–Croll theory of ferrous hydroxide precipitation during NiFe electrodeposition.

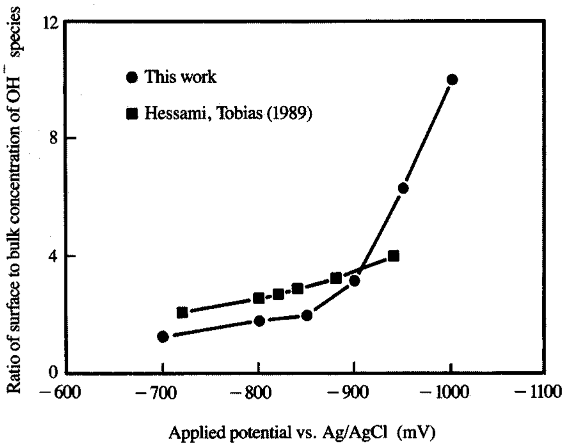

Figure 16

Comparison of theory and experiment. NiFe electrodeposition at 1600 rpm from a solution containing 0.2 M $NiCl_2$, 5 mM $FeCl_2$, and 0.4 M NaCl, and having a bulk pH of 3.

The model of Hessami and Tobias [13] predicts the dependence of the OH^- surface concentration on applied potential for a NiFe solution of pH 3. The model assumes formation of $NiOH^+$ and $FeOH^+$ species and their kinetic competition for surface sites. In **Figure 16**, we compare predicted and measured values. In the range from −700 mV to −900 mV vs. Ag/AgCl, agreement is good, with a maximum offset of only 0.2 pH units. However, at potentials more negative than −900 mV, the predicted and measured values differ considerably. The discrepancy may be due to the choice of equilibrium constants for Ni^{+2} and Fe^{+2} hydrolysis and of associated reaction constants (from the literature) because of the lack of experimental values. In essence, the predictions indicate that at a certain applied potential the surface pH should be lower than the observed values. Even though there is no full quantitative agreement between the model of Hessami and Tobias [13] and our experimental surface pH results, there is full qualitative agreement. Both indicate that NiFe anomalous deposition occurs at surface pH values much lower than those required by the Dahms–Croll mechanism. Because of the low pH values measured during NiFe deposition, formation of ferrous hydroxide at the electrode surface is not possible.

Conclusions

This study has shown that the technique described is suitable for obtaining *in situ* information about homogeneous hydrolysis and precipitation reactions which take place next to the electrode surface during metal electrodeposition. Further, it has yielded information about the mechanism of Ni electrodeposition, which appears to proceed via Ni-hydrolyzed species. When the cathode potential is driven to very negative values in a $NiCl_2$-containing solution, precipitation of a nickel hydroxychloride film $[Ni(OH)_xCl_y]$ takes place, and the formation of a metallic nickel deposit is impeded. Increased agitation maintains a low surface pH, making it possible to obtain a bright Ni deposit even without the addition of buffers. It is suggested that the presence of boric acid impedes the hydrogen evolution reaction rather than acting as a typical buffer. In addition, our measurements suggest that during NiFe electrodeposition the solution at the surface is buffered via generation of nickel and ferrous hydrolyzed species. Comparison of our measured surface pH values with the predictions of Hessami and Tobias shows relatively good agreement, therefore also suggesting that these species play an important role in the anomalous electrodeposition of NiFe.

Acknowledgments

We wish to express our appreciation to R. G. Schad for the Auger profiling work and to J. Horkans, P. C. Andricacos, and J. O. Dukovic for numerous fruitful discussions.

References

1. A. J. Bard and L. R. Faulkner, *Electrochemical Methods. Fundamentals and Applications*, John Wiley & Sons, Inc., New York, 1980.
2. A. T. Kuhn and C. Y. Chan, *J. Appl. Electrochem.* **13**, 189 (1983).
3. D. R. Eastham and P. J. Boden, *Trans-Inst. Met. Finish.* **46**, 37 (1968).
4. J. Matulis and R. Slizys, *Electrochim. Acta* **9**, 1177 (1964).
5. V. S. Kublanowski, *Teor. Eksp. Khim.* **11**, 128 (1975).
6. A. Brenner, *Electrodeposition of Alloys*, Vol. I, Academic Press, Inc., New York, 1963.
7. A. Knoedler and K. W. Neugebohren, *Metalloberflaeche* **24**, 28 (1970).
8. L. Harris, *J. Electrochem. Soc.* **120**, 1034 (1973).
9. H. Dahms and I. M. Croll, *J. Electrochem. Soc.* **112**, 771 (1965).
10. E. E. Castellani, J. V. Powers, and L. T. Romankiw, U.S. Patent 4,102,756, 1978.
11. J. V. Powers and L. T. Romankiw, U.S. Patent 3,652,442, 1972.
12. P. C. Andricacos, C. Arana, J. Tabib, J. O. Dukovic, and L. T. Romankiw, *J. Electrochem. Soc.* **136**, 1336 (1989).
13. S. Hessami and C. W. Tobias, *J. Electrochem. Soc.* **128**, 838 (1989).
14. L. T. Romankiw, Abstract 457, *The Electrochemical Society Extended Abstracts* **86-2**, 682 (1986); *Proceedings of the Symposium on Electrodeposition Technology, Theory and Practice* (L. T. Romankiw and D. R. Turner, Eds.) **87-17**, 301–325 (1987). This paper was originally presented at the 1986 Fall Meeting of The Electrochemical Society, Inc.
15. L. T. Romankiw, *IBM Tech. Disclosure Bull.* **13**, 69 (1970).
16. L. T. Romankiw, Abstract 290, *The Electrochemical Society Extended Abstracts* **70-1**, 704 (1970).
17. L. T. Romankiw, presented at SUR/FIN '90 Technical Conference, Boston, MA, 1990.
18. H. Deligianni and L. T. Romankiw, Abstract 309, *The Electrochemical Society Extended Abstracts* **89-2**, 446 (1989); *Proceedings of the Symposium on Magnetic Materials, Processing, and Devices* (L. T. Romankiw and D. A. Herman, Jr., Eds.) **90-8**, 407 (1990). This paper was originally presented at the 1989 Fall Meeting of The Electrochemical Society, Inc.
19. H. Deligianni and L. T. Romankiw, Abstract 310, *The Electrochemical Society Extended Abstracts* **89-2**, 448 (1989); *Proceedings of the Symposium on Magnetic Materials, Processing, and Devices* (L. T. Romankiw and D. A. Herman, Jr., Eds.), p. 423 (1990). This paper was originally presented at the 1989 Fall Meeting of The Electrochemical Society, Inc.
20. H. Deligianni and L. T. Romankiw, presented at the SUR/FIN '90 Technical Conference, 1990.
21. H. Deligianni and L. T. Romankiw, Abstract 343, *The Electrochemical Society Extended Abstracts* **90-2**, 498 (1990). This paper was originally presented at the 1990 Fall Meeting of The Electrochemical Society, Inc.
22. H. Deligianni and L. T. Romankiw, International Society of Electrochemistry, Abstract 2-33, 42nd Meeting, Montreaux, Switzerland, August 25–30, 1991.
23. C. F. Baes and R. E. Mesmer, *The Hydrolysis of Cations*, John Wiley & Sons, Inc., New York, 1976.
24. J. Horkans, *J. Electrochem. Soc.* **126**, 1862 (1979).

Received March 9, 1992; accepted for publication November 10, 1992

Hariklia Deligianni *IBM Technology Products, East Fishkill facility, Route 52, Hopewell Junction, New York 12533 (DELIGIAN at FSHVMX).* Dr. Deligianni is an Advisory Engineer in the Silicon Research and Development Center at the East Fishkill facility. After receiving a Ph.D. degree in chemical engineering at the University of Illinois at Urbana–Champaign, she joined IBM at the Thomas J. Watson Research Center as a Postdoctoral Fellow in the Electrochemical Technology Department. Since 1990, Dr. Deligianni has been a member of the Silicon Research and Development Center, where she has worked on the development of processes for fabricating C4 interconnections and on-chip wiring. Her research interests include thin-film electrodeposition of metals and alloys and their properties. Dr. Deligianni is a member of The Electrochemical Society and the American Institute of Chemical Engineers.

Lubomyr T. Romankiw *IBM Research Division, Thomas J. Watson Research Center, P.O. Box 218, Yorktown Heights, New York 10598 (ROMAN at YKTVMV, roman@watson.ibm.com).* Dr. Romankiw is a Senior Manager in the Electrochemical Technology Department, Manufacturing Research, at the IBM Thomas J. Watson Research Center. He received a B.Sc. in chemical engineering in 1955 from the University of Alberta, and M.Sc. and Ph.D. degrees in metallurgy and materials science in 1962 from the Massachusetts Institute of Technology. Since joining IBM in 1962, he has worked in developing dry and electrochemical fabrication processes for magnetic thin-film heads, X-ray lithography masks, bubble memory devices, silicon integrated circuits, and electronic packages. Dr. Romankiw has authored or coauthored 41 patents, more than 100 technical papers and reports, and three book chapters; he was an editor of four ECS symposium proceedings volumes. He is a member of The Electrochemical Society, the AESF, the International Society of Electrochemistry, the IEEE, the Schevchenko Scientific Society, the Ukrainian Engineers Society, Sigma Xi, and Phi Lambda Upsilon. Dr. Romankiw has earned seven IBM Outstanding Invention and Outstanding Contribution Awards and 22 IBM Invention Achievement Awards. In 1984, together with R. J. Von Gutfeld, he received the Research Award from the Electrodeposition Division of The Electrochemical Society. Dr. Romankiw was named IBM Fellow in 1986, member of the IBM Academy of Technology in 1987, and ECS Fellow in 1990; he was elected a member of the Academy of Engineering Sciences of Ukraine in 1992. He received the AESF Scientific Achievement Award in 1992, the ACS Distinguished Chemist of Westchester Award in 1993, and the Perkin Medal, also in 1993.